ELSEVIER

Int. J. Therm. Sci. 41 (2002) 147–155

International Journal of Thermal Sciences

Unsteady mhd flow and heat transfer on a rotating disk in an ambient fluid

H.S. Takhar [a,*], A.K. Singh [b], G. Nath [c]

[a] Department of Engineering and Technology, Manchester Metropolitan University, Manchester, M1 5GD, UK
[b] Department of Mathematics, Banaras Hindu University, Varansi-221005, India
[c] Department of Mathematics, Indian Institute of Science, Bangalore-550012, India

Received 2 August 2000; accepted 5 March 2001

Abstract

An unsteady flow and heat transfer of a viscous incompressible electrically conducting fluid over a rotating infinite disk in an otherwise ambient fluid are studied. The unsteadiness in the flow field is caused by the angular velocity of the disk which varies with time. The magnetic field is applied normal to the disk surface. The new self-similar solution of the Navier–Stokes and energy equations is obtained numerically. The solution obtained here is not only the solution of the Navier–Stokes equations, but also of the boundary layer equations. Also, for a simple scaling factor, it represents the solution of the flow and heat transfer in the forward stagnation-point region of a rotating sphere or over a rotating cone. The asymptotic behaviour of the solution for a large magnetic field or for a large independent variable is also examined. The surface shear stresses in the radial and tangential directions and the surface heat transfer increase as the acceleration parameter increases. Also the surface shear stress in the radial direction and the surface heat transfer decrease with increasing magnetic field, but the surface shear stress in the tangential direction increases.

Keywords: Unsteady flows; MHD flows; Rotating disk

1. Introduction

The study of the rotation of electrically conducting fluids is important in several astrophysical and geophysical situations such as the study of the terrestial magnetic field, the dynamics of rotating stars, etc. [1]. Also the study is interesting from the mathematical point of view. The system of partial differential equations with initial and boundary conditions which describe the motion can be converted into a system of ordinary differential equations with boundary conditions, if we assume a particular dependence of the coordinates for the velocity field.

Von Karman [2] was the first scientist to study the steady incompressible viscous flow over a rotating infinite disk in an ambient fluid. The analogous heat transfer problem was studied by Millsaps and Pohlhausen [3], Sparrow and Gregg [4] and Wang [5]. Sparrow and Cess [6] and Loffredo [7] have considered the effect of the magnetic field on the rotating disk problem. In the above studies a self-similar solution of the Navier–Stokes equations along with the energy equation was obtained. Recently, the self-similar solution of the Navier–Stokes equations governing the unsteady two-dimensional stagnation point flow was obtained by Ma and Hui [8] using a group-theoretic method [9]. The unsteadiness in the flow field was caused by the time-dependent velocity in the potential flow given by $u_e = Ax/t$, $A > 0$, $t > 0$.

In this analysis, we have considered the unsteady flow and heat transfer of a viscous electrically conducting fluid over an infinite disk which is rotating along its axis in an ambient fluid. The unsteadiness is caused by the time-dependent angular velocity of the disk ($\Omega = A/t$, $A > 0$, $t > 0$). The flow is assumed to be axisymmetric. A magnetic field is applied in the axial direction normal to the disk. A set of transformations is found which reduces the Navier–Stokes and the energy equations with three independent variables to a system of ordinary differential equations. These ordinary differential equations are solved numerically using a double shooting method [10]. The results are compared with those of Sparrow and Cess [6].

* Correspondence and reprints.
E-mail address: h.s.takhar@mmu.ac.uk (H.S. Takhar).

1290-0729/02/$ – see front matter
PII: S1290-0729(01)01292-3

Nomenclature

Roman symbols

A	a positive dimensionless parameter	
C	constant	
C_f	skin friction coefficient in the radial direction	
$\overline{C}_f$	skin friction coefficient in the axial direction	
C_M	dimensionless moment coefficient	
f, g, h	similarity variables defined in (9a)	
F, G, H	similarity variables defined in (22)	
Ha	Hartman number	
L	characteristic length	m
M	magnetic parameter	
Nu	Nusselt number	
p	pressure	$\text{N}\cdot\text{m}^{-2}$
P	dimensionless pressure defined in (9a)	
P_1	similarity variable defined in (22)	
Pr	Prandtl number	
Q_1	quantity of fluid pumped outward defined in (35a)	m^3
$\overline{Q}_1$	quantity of fluid pumped outward defined in (35b)	m^3
r	radial coordinate	
R	radius at a large distance	
Re	Reynolds number	
Re_m	magnetic Reynolds number	
Re_r	Reynolds number based on r	
Re_R	Reynolds number based on R	
S	similarity variable defined in (22)	
t	time	
T	temperature	K
$\overline{T}$	torque defined in (34)	
u, v, w	component velocities	$\text{m}\cdot\text{s}^{-1}$
z	axial coordinate	

Greek symbols

α	thermal diffusivity	$\text{m}^2\cdot\text{s}^{-1}$
β	coefficient of cubical expansion	K^{-1}
η	similarity variable	
θ	dimensionless temperature	
μ	dynamic viscosity	$\text{kg}\cdot\text{s}^{-1}\cdot\text{m}^{-1}$
ν	kinematic viscosity	$\text{m}^2\cdot\text{s}^{-1}$
ξ	similarity variable defined in (22)	
τ	shear stress	$\text{N}\cdot\text{m}^{-2}$
Ω	time-dependant angular velocity	$\text{rad}\cdot\text{s}^{-1}$
Ω_0	initial angular velocity	$\text{rad}\cdot\text{s}^{-1}$

Subscripts

0	denotes the parameters used in (21)
1	denotes the parameter used in the asymptotic analysis
i	denotes the initial conditions
r	values of the parameters based on the radius r
R	values of the parameters based on the radius R
w	denotes the conditions at the wall
∞	denotes the conditions at infinity

2. Problem formulation

Let us consider the unsteady motion of a viscous, incompressible electrically conducting fluid over an infinite disk which is rotating with an angular velocity inversely proportional to time ($\Omega = A/t$; $A > 0$, $t > 0$) in an otherwise ambient fluid. Fig. 1 shows the flow model and the cylindrical polar coordinate system, r, ϕ and z. The flow is assumed to be axisymmetric. Hence the velocity components u, v, w and the temperature T are independent of ϕ. A uniform magnetic field of strength B is applied in the z-direction. It is assumed that the magnetic Reynolds number $Re_m = \mu_0 \sigma VL \ll 1$, where μ_0 is the magnetic permeability, σ is the electrical conductivity and V and L are, respectively, the characteristic velocity and length. Under this condition it is possible to neglect the induced magnetic field in comparison to the applied magnetic field. The wall temperature T_w and the ambient temperature T_∞ are assumed to be constant. The effects of viscous dissipation and Ohmic heating are neglected. Under the above-mentioned assumptions, the Navier–Stokes equations and the energy equation governing the unsteady MHD viscous axisymmetric flow over a rotating infinite insulated disk are are given by [6,11],

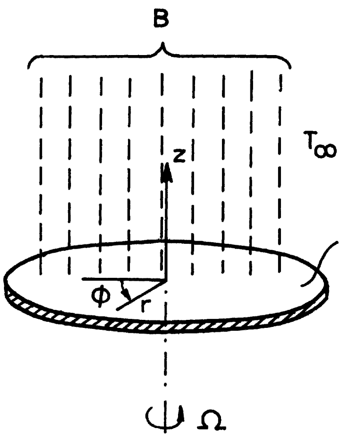

Fig. 1. Physical model and coordinate system.

$$\frac{\partial}{\partial r}(ru) + \frac{\partial}{\partial z}(rw) = 0 \tag{1}$$

$$\frac{\partial u}{\partial t} + u\frac{\partial u}{\partial r} + w\frac{\partial u}{\partial z} - \frac{v^2}{r} = -\rho^{-1}\frac{\partial p}{\partial r} - \frac{\sigma B^2 u}{\rho} + \nu\left(\nabla^2 u - \frac{u}{r^2}\right) \tag{2}$$

$$\frac{\partial v}{\partial t}+u\frac{\partial v}{\partial r}+w\frac{\partial v}{\partial z}+\frac{uv}{r}=-\frac{\sigma B^2 v}{\rho}+\nu\left(\nabla^2 v-\frac{v}{r^2}\right) \quad (3)$$

$$\frac{\partial w}{\partial t}+u\frac{\partial w}{\partial r}+w\frac{\partial w}{\partial z}=-\rho^{-1}\frac{\partial p}{\partial z}+\nu\nabla^2 w \quad (4)$$

$$\frac{\partial T}{\partial t}+u\frac{\partial T}{\partial r}+w\frac{\partial T}{\partial z}=\alpha\nabla^2 T \quad (5)$$

where

$$\nabla^2=\partial^2/\partial r^2+r^{-1}\partial/\partial r+\partial^2/\partial z^2 \quad (6)$$

The initial conditions are given by

$$\begin{aligned} &u(r,z,0)=u_i(r,z)\\ &v(r,z,0)=v_i(r,z)\\ &w(r,z,0)=w_i(r,z)\\ &T(r,z,0)=T_i(r,z)\\ &p(r,z,0)=p_i(r,z) \end{aligned} \quad (7)$$

The boundary conditions are given by

$$\begin{aligned} &u(r,0,t)=0\\ &v(r,0,t)=\Omega r\\ &w(r,0,t)=p(r,0,t)=0\\ &T(r,0,t)=T_{\mathrm{w}}\\ &u(r,\infty,t)=v(r,\infty,t)=0\\ &T(r,\infty,t)=T_\infty \end{aligned} \quad (8)$$

Here u, v, w are the velocity components along the r, ϕ, z directions, respectively, t is the time, p and T are the static pressure and temperature, respectively, ρ and ν are the density and kinematic viscosity, respectively, α is the thermal diffusivity, B is the magnetic field applied in the axial (z) direction, the subscript i denotes initial conditions and the subscripts w and ∞ denote conditions at the wall and in the ambient fluid, respectively.

The partial differential equations (1)–(6) under the initial and boundary conditions (7) and (8) admit a self-similar solution if we apply the transformations given by;

$$\begin{aligned} &\eta=z(\nu t)^{-1/2},\quad \Omega=A/t,\quad A>0,\ t>0\\ &u=(Ar/t)f(\eta)\\ &v=(Ar/t)g(\eta)\\ &w=A(\nu/t)^{1/2}h(\eta)\\ &\theta(\eta)=(T-T_{\mathrm{w}})/(T_{\mathrm{w}}-T_\infty)\\ &Pr=\nu/\alpha\\ &p=\mu(A/t)P(\eta)\\ &M=Ha^2/Re_r\\ &Ha^2=\sigma B^2r^2/\mu\\ &Re_r=\Omega r^2/\nu \end{aligned} \quad (9a)$$

to Eqs. (1)–(5). It is found that Eq. (1) yields the relation

$$2f+h'=0 \quad (9b)$$

and Eqs. (2)–(5) after using (9a) reduce to

$$h'''-A\left(hh''-2^{-1}h'^2+2g^2+Mh'\right)+\left(h'+2^{-1}\eta h''\right)=0 \quad (10)$$

$$g''-A\left(hg'-h'g+Mg\right)+\left(g+2^{-1}\eta g'\right)=0 \quad (11)$$

$$Pr^{-1}\theta''-Ah\theta'+2^{-1}\eta\theta'=0 \quad (12)$$

$$P'=h''-Ahh'+h+2^{-1}\eta h' \quad (13)$$

The boundary conditions (8) can be expressed as;

$$\begin{aligned} &h=h'=0,\quad g=\theta=1,\quad P=0\quad \text{at } \eta=0\\ &h'\to 0,\quad g\to 0,\quad \theta\to 0,\quad \text{as } \eta\to\infty \end{aligned} \quad (14)$$

After Eqs. (10) and (11) have been solved, pressure P from (13) can be obtained by using the condition on P from (14) and it is given by

$$P=h'-2^{-1}Ah^2+2^{-1}\eta h+2^{-1}\int_0^\eta h\,\mathrm{d}\eta \quad (15)$$

Here η is the transformed variable, h, h' and g are, respectively, the dimensionless axial, radial and tangential velocity components, θ is the dimensionless temperature, P is the dimensionless pressure, M is the magnetic parameter, Ha is the Hartmann number, Re_r is the Reynolds number with respect to the radius r, Pr is the Prandtl number, μ is the coefficient of viscosity, and a prime denotes derivative with respect to η. A is a positive dimensionless constant which measures the reduction or an increase in the angular velocity as A decreases or increases.

Eqs. (10)–(13) represent the self-similar equations of the unsteady Navier–Stokes equations or boundary layer equations along with the energy equation. However, for boundary layer equations, the equation for pressure (13) or (15) is not required as it is assumed to be constant across the boundary layer. The steady state equations are obtained from (10)–(13) by omitting the terms due to unsteadiness and these are expressed as

$$h'''-A\left(hh''-2^{-1}h'^2+2g^2+Mh'\right)=0 \quad (16)$$

$$g''-A\left(hg'-h'g+Mg\right)=0 \quad (17)$$

$$Pr^{-1}\theta''-Ah\theta'=0 \quad (18)$$

$$P'=h''-Ahh' \quad (19)$$

The boundary conditions for the above equations are given by (14). Eq. (19) after integration and using the condition on P can be written as

$$P=h'-2^{-1}Ah^2 \quad (20)$$

Eqs. (16)–(20) for $A=1$ are identical to those of Sparrow and Cess [6].

It may be remarked that Eqs. (10)–(13) under the boundary conditions (14) and the corresponding steady-state equations also represent the flow over a rotating sphere at the forward stagnation point or over a rotating cone by a simple change in the scaling factor.

For a sphere rotating in an ambient fluid, we use the transformations;

$$\begin{aligned} &\eta=2^{-1/2}\eta_0\\ &h(\eta)=-2^{1/2}h_0(\eta_0)\\ &g(\eta)=g_0(\eta_0)\\ &\theta(\eta)=\theta_0(\eta_0)\\ &P(\eta)=P_0(\eta_0) \end{aligned} \quad (21)$$

For a cone rotating in an ambient fluid, the transformations (21) hold good except that $h(\eta) = -2h_0(\eta_0)$.

It is also possible to obtain a self-similar solution of Eqs. (1)–(5) for a slightly different variation of the angular velocity Ω with time, i.e., $\Omega = \Omega_0(1-\lambda t^*)^{-1}$, $t^* = \Omega_0 t$. In this case, we apply the following transformations,

$$\begin{aligned}
&\xi = (\Omega_0/\nu)^{1/2}\big(1-\lambda t^*\big)^{-1/2} z, \quad t^* = \Omega_0 t,\ \lambda t^* < 1\\
&u = \Omega_0 r\big(1-\lambda t^*\big)^{-1} F(\xi)\\
&v = \Omega_0 r\big(1-\lambda t^*\big)^{-1} G(\xi)\\
&w = (\Omega_0/\nu)^{1/2}\big(1-\lambda t^*\big)^{-1/2} H(\xi)\\
&p = \mu\Omega_0\big(1-\lambda t^*\big)^{-1} P_1(\xi)\\
&S(\xi) = (T - T_\infty)/(T_{\mathrm{w}} - T_\infty)\\
&M = Ha^2/Re_r\\
&Ha^2 = \sigma B^2 r^2/\mu\\
&Re_r = \Omega r^2/\nu
\end{aligned} \tag{22}$$

to Eqs. (1)–(5) and we find that Eq. (1) gives the relation between F and H' in the form

$$2F + H' = 0 \tag{23}$$

and Eqs. (2)–(5) after using (23) reduce to the following,

$$\begin{aligned}
&\frac{\mathrm{d}^3H}{\mathrm{d}\xi^3} - H\frac{\mathrm{d}^2H}{\mathrm{d}\xi^2} + 2^{-1}\left(\frac{\mathrm{d}H}{\mathrm{d}\xi}\right)^2 - 2G^2\\
&\quad - M\frac{\mathrm{d}H}{\mathrm{d}\xi} - \lambda\left(\frac{\mathrm{d}H}{\mathrm{d}\xi} + 2^{-1}\xi\frac{\mathrm{d}^2H}{\mathrm{d}\xi^2}\right) = 0
\end{aligned} \tag{24}$$

$$\frac{\mathrm{d}^2G}{\mathrm{d}\xi^2} - H\frac{\mathrm{d}G}{\mathrm{d}\xi} + \frac{\mathrm{d}H}{\mathrm{d}\xi}G - MG - \lambda\left(G + 2^{-1}\xi\frac{\mathrm{d}G}{\mathrm{d}\xi}\right) = 0 \tag{25}$$

$$Pr^{-1}\frac{\mathrm{d}^2S}{\mathrm{d}\xi^2} - H\frac{\mathrm{d}S}{\mathrm{d}\xi} - 2^{-1}\lambda\xi\frac{\mathrm{d}S}{\mathrm{d}\xi} = 0 \tag{26}$$

$$\frac{\mathrm{d}P_1}{\mathrm{d}\xi} = \frac{\mathrm{d}^2H}{\mathrm{d}\xi^2} - H\frac{\mathrm{d}H}{\mathrm{d}\xi} - 2^{-1}\lambda\left(H + \xi\frac{\mathrm{d}H}{\mathrm{d}\xi}\right) \tag{27}$$

The boundary conditions are given by

$$\begin{aligned}
&H = \mathrm{d}H/\mathrm{d}\xi = P_1 = 0, \quad G = S = 1 \quad \text{at } \xi = 0\\
&\mathrm{d}H/\mathrm{d}\xi \to 0, \quad G \to 0, \quad S \to 0 \quad \text{as } \xi \to \infty
\end{aligned} \tag{28}$$

The system of Eqs. (24)–(28) represents the unsteady flow and the corresponding steady flow equations are obtained by putting $\lambda = 0$ in these equations. Also Eqs. (10)–(13) can be transformed to Eqs. (25)–(27) by using the following transformations,

$$\begin{aligned}
&\eta = A^{-1/2}\xi\\
&h(\eta) = A^{-1/2}H(\xi)\\
&g(\eta) = G(\xi)\\
&\theta(\eta) = S(\xi)\\
&P(\eta) = P_1(\xi)\\
&A = -(\lambda)^{-1}, \quad \lambda < 0
\end{aligned} \tag{29}$$

The skin friction coefficients in the radial and tangential directions C_{f} and $\overline{C}_{\mathrm{f}}$ (i.e., in the r and z directions) can be written as

$$\begin{aligned}
C_{\mathrm{f}} &= -2\mu(\partial u/\partial z)_{z=0}/\rho r^2\Omega^2\\
&= -2\,Re_r^{-1/2}A^{-1/2}h''(0)
\end{aligned} \tag{30}$$

$$\begin{aligned}
\overline{C}_{\mathrm{f}} &= -2\mu(\partial v/\partial z)_{z=0}/\rho r^2\Omega^2\\
&= -2\,Re_r^{-1/2}A^{-1/2}g'(0)
\end{aligned} \tag{31}$$

The heat transfer coefficient in terms of the Nusselt number Nu can be expressed as

$$Nu = -r(\partial T/\partial z)_{z=0}/(T_{\mathrm{w}} - T_\infty) = -A^{-1/2}\,Re_r^{1/2}\theta'(0) \tag{32}$$

It may be remarked that the results here are strictly valid for an infinite disk only. However, it is possible to utilize the same results for a finite disk provided its radius R is large compared with the thickness δ of the layer carried with the disk. The dimensionless moment coefficient C_{M} for a disk of large but finite radius R is expressed as,

$$C_{\mathrm{M}} = 4\overline{T}/\big(\rho\Omega^2R^5\big) = -2\pi\,Re_R^{-1/2}A^{-1/2}g'(0) \tag{33}$$

where

$$\begin{aligned}
&\overline{T} = -2\pi\int_0^R \mu(\partial v/\partial z)_{z=0}r^2\,\mathrm{d}r\\
&Re_R = \Omega R^2/\nu
\end{aligned} \tag{34}$$

The quantity of fluid Q_1 which is pumped outwards due to the centrifugal force on one side of the disk of radius R is given by,

$$Q_1 = 2\pi R\int_0^\infty u\,\mathrm{d}z = -\pi\Omega R^3\,Re_R^{-1/2}h(\infty) \tag{35a}$$

In dimensionless form it can be written as

$$\overline{Q}_1 = Q_1/\big(\Omega R^3\big) = -2\pi\,Re_R^{-1/2}h(\infty) \tag{35b}$$

Here $\overline{T}$ is the torque, Re_R is the Reynolds number with respect to the radius R, $h(\infty)$ is the dimensionless ambient velocity and $\overline{Q}_1$ is the amount of fluid being pumped outwards.

3. Asymptotic solution for large η

Here we consider the asymptotic behaviour of the solution of Eqs. (10)–(12) under the conditions (14) for large values of the independent variable η. As $\eta \to \infty$, $h' \to 0$, $g \to 0$, $\theta \to 0$. Hence $h \to -C$, ($C > 0$) as $\eta \to \infty$. The justification for taking $h < 0$ is that the numerical solution of (10) and (11) shows that $h < 0$ for all η. Therefore, we set for large η

$$\begin{aligned}
&h(\eta) = -C + h_1(\eta)\\
&g(\eta) = g_1(\eta)\\
&\theta(\eta) = \theta_1(\eta)
\end{aligned} \tag{36}$$

where h_1 and g_1 and θ_1 are small and hence their squares and products can be neglected. Using (36) in Eqs. (10)–(12), we can obtain,

$$h_1''' + (2^{-1}\eta + AC)h_1'' - (AM-1)h_1' = 0 \tag{37a}$$

$$g_1'' + (2^{-1}\eta + AC)g_1' - (AM-1)g_1 = 0 \tag{37b}$$

$$\theta_1'' + Pr(2^{-1}\eta + AC)\theta_1' = 0 \tag{37c}$$

By changing the independent variable from η to η_1, where

$$\eta_1 = 2^{1/2}(2^{-1}\eta + AC) \tag{38}$$

Eqs. (37a)–(37b) can be re-written as

$$\frac{d^3h_1}{d\eta_1^3} + \eta_1\frac{d^2h_1}{d\eta_1^2} - 2(AM-1)\frac{dh_1}{d\eta_1} = 0 \tag{39a}$$

$$\frac{d^2g_1}{d\eta_1^2} + \eta_1\frac{dg_1}{d\eta_1} - 2(AM-1)g_1 = 0 \tag{39b}$$

$$\frac{d^2\theta_1}{d\eta_1^2} + Pr\,\eta_1\frac{d\theta_1}{d\eta_1} = 0 \tag{39c}$$

with the boundary conditions

$$\frac{dh_1}{d\eta_1} \to 0, \quad g_1 \to 0, \quad \theta_1 \to 0, \quad \text{as } \eta_1 \to \infty \tag{40}$$

The solutions of (39a)–(39b) under the boundary conditions (40) can be expressed as [12];

$$2^{1/2}\frac{dh}{d\eta} = g = \frac{dh_1}{d\eta_1} = g_1 = b_1 \exp(-\eta_1^2/2)(\eta_1)^{-(2AM-1)} \times [1 + 0(\eta_1^{-2})] \tag{41a}$$

$$\theta = \theta_1 = -b_2(Pr\,\eta_1)^{-1}\exp(-Pr\,\eta_1^2/2) \times [1 - (Pr\,\eta_1^2)^{-1} + O(\eta_1^{-4})] \tag{41b}$$

When $AM = 1$, the solutions of Eqs. (39a) and (39b) under the conditions (40) are given by,

$$2^{1/2}\frac{dh}{d\eta} = g = \frac{dh_1}{d\eta_1} = g_1 = -b_3(\eta_1)^{-1}\exp(-\eta_1^2/2) \times [1 - \eta_1^{-2} + O(\eta_1^{-4})] \tag{42}$$

where b_1, b_2 and b_3 are arbitrary constants. The above equations show that for $AM > 0.5$, $dh/d\eta$, g and θ decay exponentially as $\eta_1 \to \infty$.

4. Approximate solutions for large M

It is possible to obtain an approximate closed form solutions of Eqs. (10)–(12) under conditions (14) for large values of the magnetic parameter M ($M > 3$). The numerical results show that both h and h' (i.e., axial and radial velocity components) become vary small for large M.

Using this, Eq. (11) is reduced to

$$g'' + 2^{-1}\eta g' - (AM-1)g = 0 \tag{43}$$

The solution of Eq. (43) under the boundary conditions (14) can be expressed in the form [12]

$$g = \exp(-3\eta^2/16)\left[{}_1F_1\left(\frac{4AM-1}{8}, \frac{1}{2}, \frac{\eta^2}{8}\right) + \left(\frac{b_5}{b_4}\right)\eta_1 F_1\left(\frac{4AM+3}{8}, \frac{3}{2}, \frac{\eta^2}{8}\right)\right] \tag{44}$$

Hence

$$g'(0) = b_5/b_4 \tag{45}$$

where

$$b_4 = \Gamma(1/3)/\Gamma(3+4AM)/8$$

$$b_5 = 2^{-1/2}\Gamma(-1/3)/\Gamma(4AM-1)/8$$

$${}_1F_1(a,c,x) = \sum_{j=0}^{\infty} C_j x^j$$

$$C_j = \frac{a(a+1)\cdots(a+j-1)}{c(c+1)\cdots(c+j-1)}\frac{1}{j_i}$$

$${}_1F_1(1+a-c, 2-c, x) = \sum_{j=0}^{\infty} D_j x^j$$

$$D_j = \frac{(1+a-c)(2+a-c)\cdots(1+a-c+j-1)}{(2-c)(3-c)\cdots(2-c+j-1)}\frac{1}{j_i}$$

$$a = (4AM-1)/8, \qquad c = 1/2, \qquad x = \eta^2/8 \tag{46}$$

Here ${}_1F_1\,(a,c,x)$ is the confluent hypergeometric series and Γ denotes the gamma function.

For large values of the magnetic parameter M, the thermal boundary layer is much thicker than the velocity boundary layer. Under this condition, we can write

$$h(\eta) \approx h(\infty) = \text{constant}, \quad h(\infty) < 0 \tag{47}$$

Using relations (47) in (12), we obtain,

$$\theta'' + Pr[2^{-1}\eta + A(-h(\infty))]\theta' = 0 \tag{48}$$

The solution of Eq. (48) under the boundary conditions (14) can be expressed as

$$\theta = 1 - \left[\int_0^\eta Q(x)\,dx \Big/ \int_0^\infty Q(x)\,dx\right] \tag{49}$$

where

$$Q(x) = \exp[-Pr(x^2/4 + A(-h(\infty))x)] \tag{50}$$

Under the condition that h and h' are very small for large M, Eq. (11) reduces to

$$h''' + 2^{-1}\eta h'' - (AM-1)h' = 2Ag^2 \tag{51}$$

Eq. (51) is a linear non-homogenous equation and its solution under conditions (14) can be expressed in the form [12]

$$h' = -2A\exp(-3\eta^2/16) \times \left[{}_1F_1\left(\frac{4AM-1}{8}, \frac{1}{2}, \frac{\eta^2}{8}\right)\right.$$

$$+\left(\frac{b_5}{b_4}\right)\eta_1 F_1\left(\frac{4AM+3}{8},\frac{3}{2},\frac{\eta^2}{8}\right)\Bigg]$$
$$+2A\exp\left(-2\eta^2/8\right)$$
$$\times\Bigg[1+2\left(\frac{b_5}{b_4}\right)\eta+\left(\frac{4AM+3}{8}\right)\eta^2$$
$$+\left(\frac{4AM+7}{12}\right)\left(\frac{b_5}{b_4}\right)\eta^3$$
$$+\frac{1}{12}\left(\frac{4AM-1}{16}+\frac{(4AM+3)(4AM+7)}{32}\right.$$
$$\left.+\left(\frac{b_5}{b_4}\right)^2\right)\eta^4\Bigg] \tag{52}$$

Hence

$$h''(0)=2Ab_5/b_4 \tag{53}$$

For $AM = 1$, the solution of Eq. (43) under the conditions (14) reduces to a simple form

$$g=\operatorname{erfc}(\eta/2),\quad g'(0)=-1/(\pi)^{1/2} \tag{54}$$

The results of this approximate closed-form method for $M \geqslant 3$, $0.5 \leqslant A \leqslant 2$ are in good agreement with those obtained by using the numerical method. For $M = 3$, $A = 1$, $-h''(0)$ and $-g'(0)$ differ by about 2% and $-\theta'(0)$ by about 4% (when $Pr = 0.7$). For larger M or for smaller Pr (in the case of heat transfer), this difference decreases.

5. Results and discussion

Eqs. (10)–(12) under the boundary conditions (14) have been solved numerically using a double shooting method which is described in detail in [10]. The results are obtained for various values of the parameters M and A.

In order to assess the accuracy of our method, we have compared our steady-state results obtained from Eqs. (16)–(18) under the boundary conditions (14) for $A = Pr = 1$ with those of Sparrow and Cess [6]. The results are found to be in excellent agreement. The maximum difference is less than 0.2%. Since the results are given by Sparrow and Cess [6] in Tables 1 and 2, these are not presented here.

The effect of the magnetic parameter M on the velocity profiles in the radial, tangential and axial directions $-h'(\eta)$, $g(\eta)$, $-h(\eta)$ and on the temperature profiles $g(\eta)$ for $A = 1$, $Pr = 0.7$ is shown in Figs. 2–5. The rotating disk acts like a fan drawing fluid axially inwards from the surroundings toward the disk surface. Since the disk is nonporous the

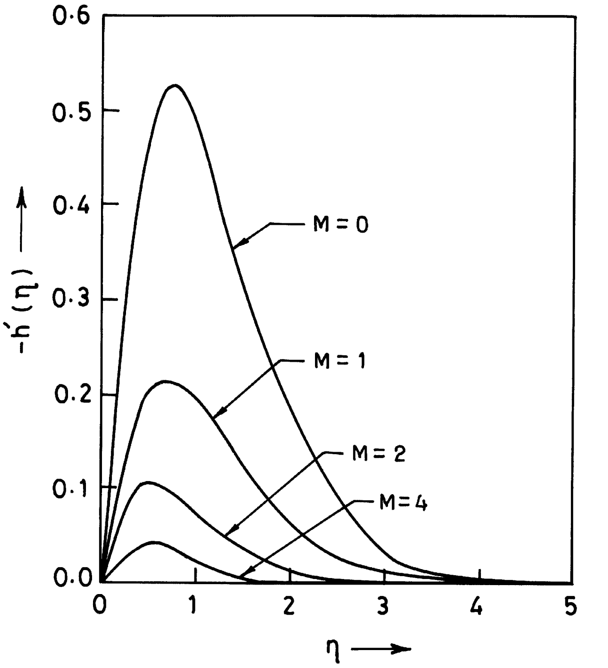

Fig. 2. Velocity profiles in the radial direction, $-h'(\eta)$, for $A = 1$, $0 \leqslant M \leqslant 4$.

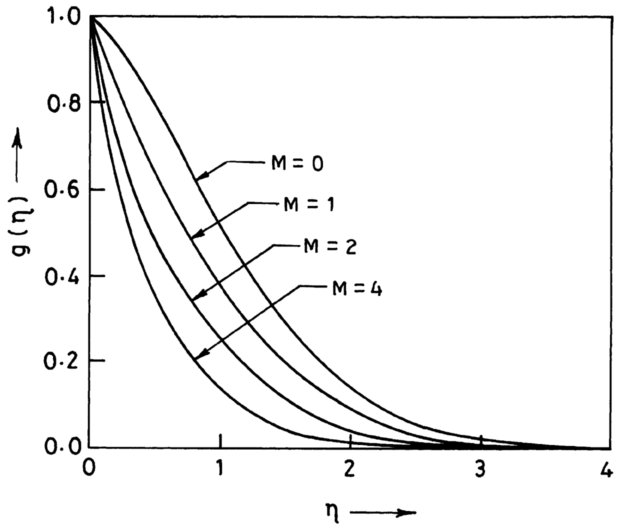

Fig. 3. Velocity profiles in the tangential direction, $g(\eta)$, for $A = 1$, $0 \leqslant M \leqslant 4$.

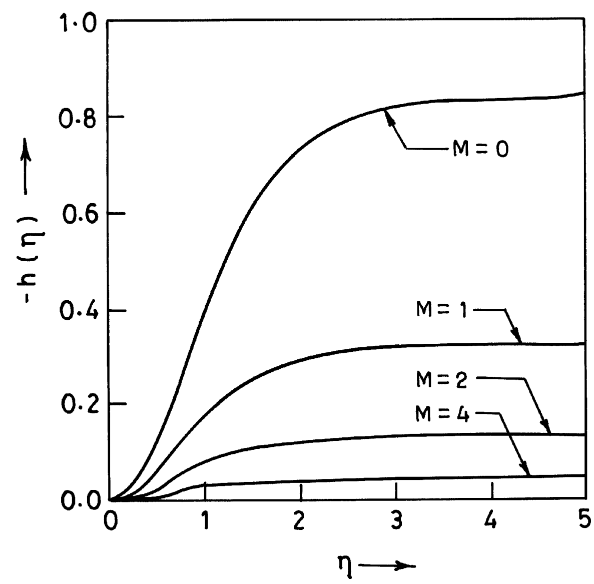

Fig. 4. Velocity profiles in the axial direction, $-h(\eta)$, for $A = 1$, $0 \leqslant M \leqslant 4$.

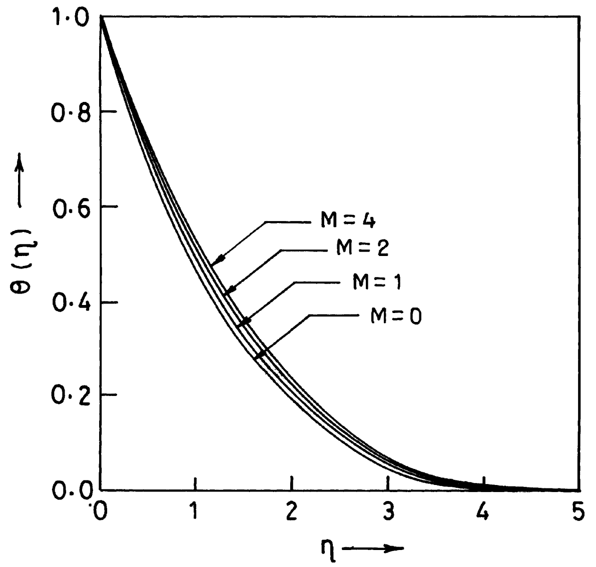

Fig. 5. Temperature profiles, $\theta(\eta)$, for $A = 1$, $Pr = 0.7$, $0 \leqslant M \leqslant 4$.

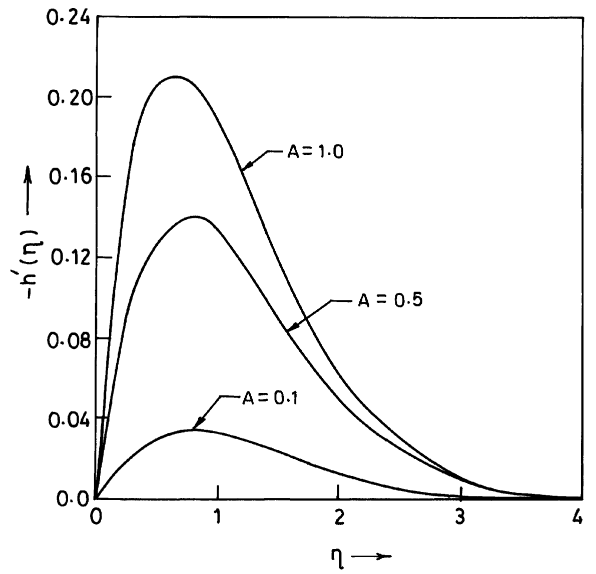

Fig. 6. Velocity profiles in the radial direction, $-h'(\eta)$, for $M = 1$, $0.1 \leqslant A \leqslant 1$.

inflowing fluid is turned away and discharges in the radial direction. Hence there is a close correlation between the axial inflow and the radial outflow. Here the magnetic field is applied in the axial direction. Hence there is no magnetic force to retard the axial velocity $h(\eta)$, but there is a radial component of the magnetic force which opposes the radial velocity $h'(\eta)$. Hence the reduction in the radial velocity is reflected as a reduction in the incoming axial velocity. Since there is less fluid flow, the turning from axial to radial velocity occurs near the surface of the disk. Hence the axial velocity $h(\eta)$ is constant near the disk surface as the magnetic parameter M increases. Hence there is a significant reduction in radial and axial velocities as M increases (Figs. 2 and 4). The magnetic field B also gives rise to the magnetic force in the tangential direction which

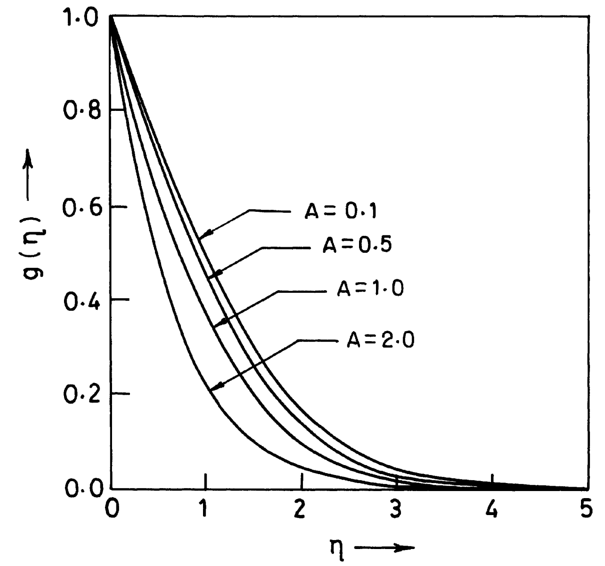

Fig. 7. Velocity profiles in the tangential direction, $g(\eta)$, for $M = 1$, $0.1 \leqslant A \leqslant 2$.

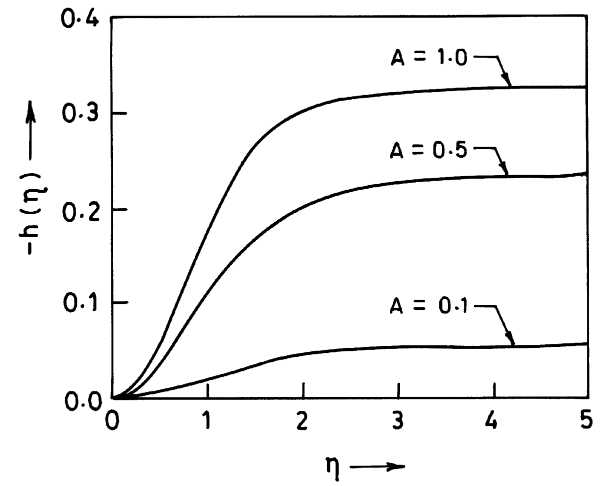

Fig. 8. Velocity profiles in the axial direction, $-h(\eta)$, for $M = 1$, $0.1 \leqslant A \leqslant 1$.

opposes the tangential flow velocity $g(\eta)$. Consequently, the tangential velocity is everywhere lowered and the boundary layer thickness is reduced which is evident from Fig. 3.

From Fig. 5, it can be seen that the temperature and the thermal boundary layer thickness increase with M. The reason for this trend is that the axial velocity h decreases with increasing M. However, the effect of M on the temperature profiles $\theta(\eta)$ is not very significant, because the magnetic parameter M does not explicitly occur in the energy equation.

The effect of the acceleration (deceleration) parameter A on the radial, tangential and axial velocity profiles $-h'(\eta)$, $g(\eta)$, $-h(\eta)$ and on the temperature profiles $\theta(\eta)$ for $M = 1$, $Pr = 0.7$ is presented in Figs. 6–9. From these figures it is evident that the radial velocity $-h'(\eta)$, and the axial velocity, $-h(\eta)$, increase everywhere as A increases, but the tangential velocity, $g(\eta)$, and the

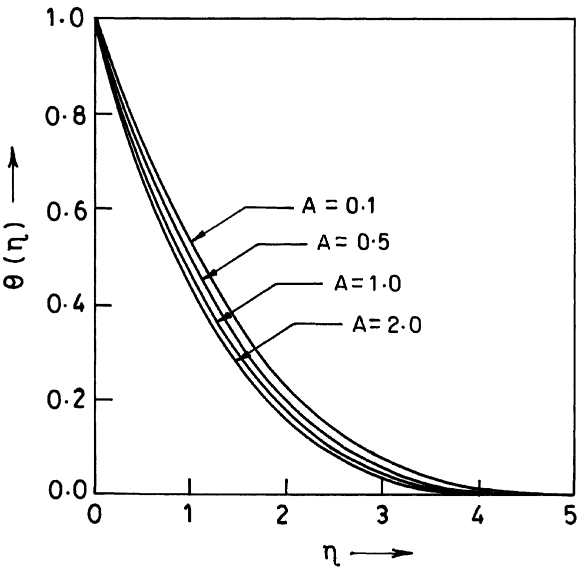

Fig. 9. Temperature profiles, $\theta(\eta)$, for $M = 1$, $Pr = 0.7$, $0.1 \leqslant A \leqslant 2$.

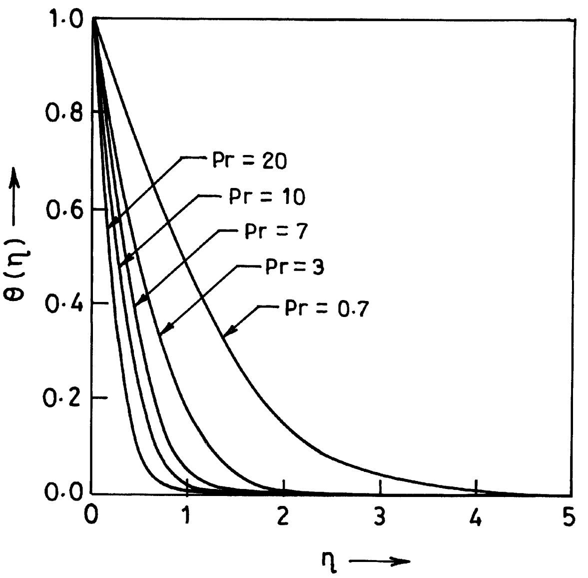

Fig. 10. Temperature profiles, $\theta(\eta)$, for $M = A = 1$, $0.7 \leqslant Pr \leqslant 20$.

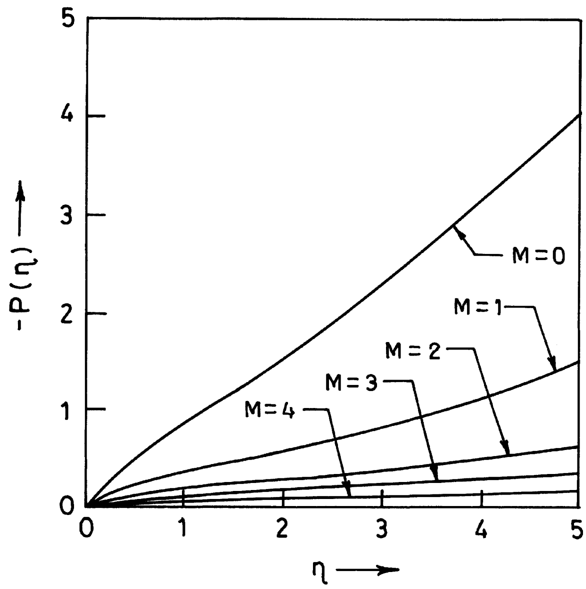

Fig. 11. Pressure profiles, $P(\eta)$, for $A = 1$, $0 \leqslant M \leqslant 4$.

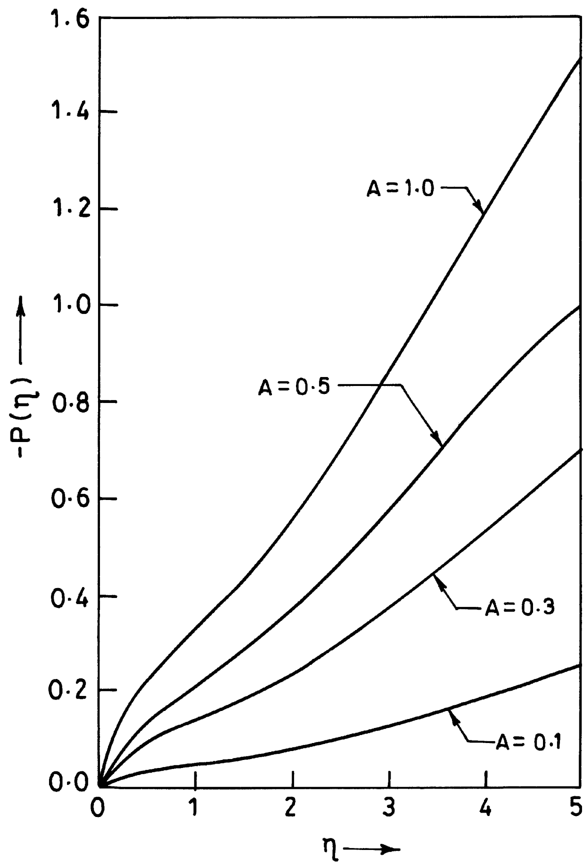

Fig. 12. Pressure profiles, $P(\eta)$, for $M = 1$, $0.1 \leqslant A \leqslant 1$.

temperature, $\theta(\eta)$, are reduced. The physical reason for this behaviour is that an increase in A implies an increase in the angular velocity which imports additional momentum into the boundary layer. This increases the axial inflow and the radial outflow. Consequently, both the radial and axial velocities increase with A. Further, the tangential velocity g(η) and the temperature ($\theta(\eta)$) are reduced and their gradients increase with increasing A.

The effect of the Prandtl number *Pr* on the temperature profiles $\theta(\eta)$ for $A = M = 1$ is displayed in Fig. 10. Since the thermal boundary layer significantly reduces with increasing *Pr*, there is a significant reduction in temperature everywhere.

Fig. 11 shows the effect of the magnetic parameter M on the dimensionless pressure profiles $P(\eta)$ for $A = 1$. Since P depends on the radial and axial velocities $h'(\eta)$, $h(\eta)$ which decrease with increasing M, the pressure P decreases with increasing M.

In Fig. 12 the effect of the acceleration parameter A on $P(\eta)$ for $M = 1$ is presented. $P(\eta)$ is found to increase

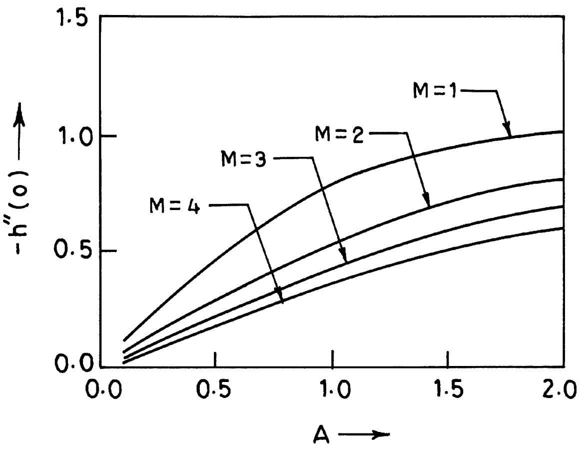

Fig. 13. Variation of the surface shear stress in the radial direction, $-h''(0)$, with the acceleration parameter A for $0 \leqslant M \leqslant 4$.

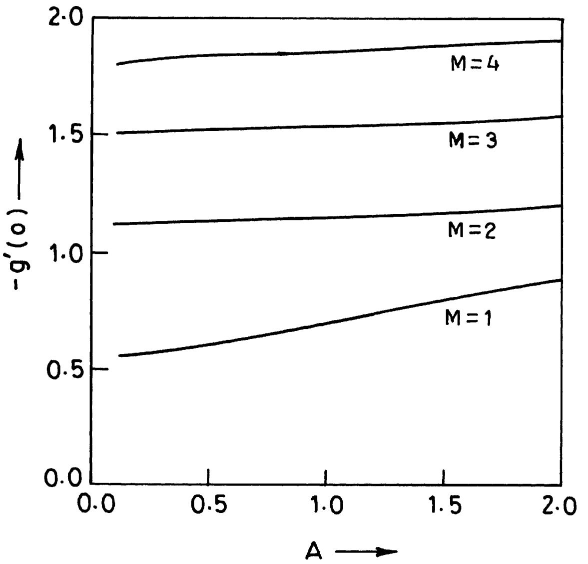

Fig. 14. Variation of the surface shear stress in the tangential direction, $-g'(0)$, with the acceleration parameter A for $0 \leqslant M \leqslant 4$.

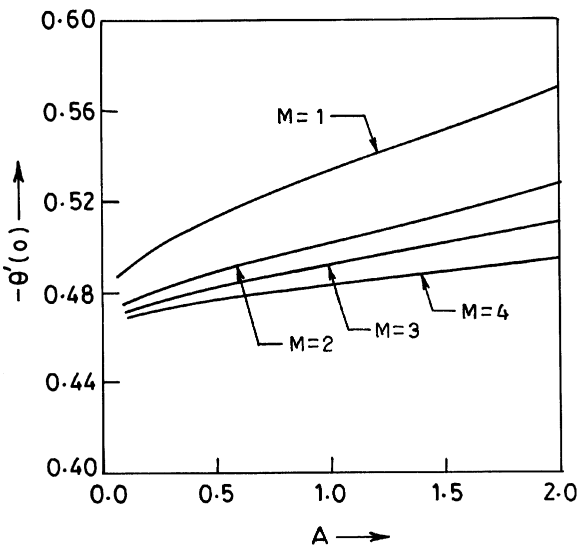

Fig. 15. Variation of the surface heat transfer, $-\theta'(0)$, with the acceleration parameter A for $0 \leqslant M \leqslant 4$, $Pr = 0.7$.

with A, since the axial and radial velocities (h, h') increase with A.

The variation of the surface shear stresses on the radial and tangential directions $-h'(0)$, $-g(0)$ and the surface heat transfer $-\theta'(0)$ with A for $1 \leqslant M \leqslant 4$, $Pr = 0.7$ is, shown in Figs. 13–15, respectively. For a fixed M, they all increase with A, since an increase in A enhances the angular velocity of the disk which accelerates the fluid near the surface. Also for a fixed A, the shear stress in the radial direction $-h''(0)$ and the heat transfer $-\theta'(0)$ decrease with increasing M, but the surface shear stress in the tangential direction increases. The reason for this trend has been explained earlier.

6. Conclusions

A new self-similar solution of the Navier–Stokes equations along with the energy equation governing the unsteady viscous MHD flow over an infinite disk rotating in an ambient fluid has been obtained. By a simple scaling, it also represents the solution over a rotating sphere at the forward stagnation point (or over a rotating cone). There is a significant reduction in the radial and axial velocity components due to an increase in the magnetic field, but the tangential velocity increases. Also the surface shear stress in the radial direction and the heat transfer decrease with an increasing magnetic field, but the surface shear stress in the tangential direction increases. However, they all increase with the increasing acceleration parameter.

References

[1] E.N. Parker, Cosmical Magnetic Fields, Clarenden Press, Oxford, 1979.

[2] Th. von Karman, Uber laminare und tubulente Reibung, J. Agnew. Math. Mech. 1 (1921) 233–252.

[3] K.M. Millsaps, K. Pohlhausen, Heat transfer by laminar flow from a rotating disk, J. Aeronaut. Sci. 19 (1952) 120–136.

[4] E.M. Sparrow, J.L. Gregg, Heat transfer from a rotating disk in fluids of any Prandtl number, ASME J. Heat Transfer. 81 (1959) 240–251.

[5] C.Y. Wang, Boundary layers on rotating cones, disks and axisymmetric surfaces with a concentrated heat source, Acta Mech. 81 (1990) 245–251.

[6] E.M. Sparrow, R.D. Cess, Magnetohydrodynamic flow and heat transfer about a rotating disk, ASME J. Appl. Mech. 29 (1962) 181–187.

[7] M.I. Loffredo, Extension of von Karman ansatz to magnetohydrodynamics, Meccanica 21 (1986) 81–86.

[8] P.K.H. Ma, M.A. Hui, Similarity solutions of the two-dimensional unsteady boundary layer equations, J. Fluid Mech. 216 (1990) 537–559.

[9] P.J. Oliver, Applications of Lie Groups to Differential Equations, Springer, Berlin, 1986.

[10] H.S. Takhar, Free convection from a flat plate, J. Fluid Mech. 84 (1968) 9.

[11] A.C. Eringen, G.A. Maugin, Electodynamics of Continua, Vol. 2, Springer, Berlin, 1990.

[12] E.T. Whittaker, G.N. Watson, Modern Analysis, Cambridge University Press, London, 1963.